



Citation for published version:

Shi, S, Collins, L, Mahon, M, Djurovich, P, Thompson, M & Whittlesey, M 2017, 'Synthesis and characterization of phosphorescent two coordinate copper(I) complexes bearing diamidocarbene ligands', *Dalton Transactions*, vol. 46, no. 3, pp. 745-752. <https://doi.org/10.1039/C6DT04016K>

DOI:

[10.1039/C6DT04016K](https://doi.org/10.1039/C6DT04016K)

Publication date:

2017

Document Version

Peer reviewed version

[Link to publication](#)

The final publication is available at the Royal Society of Chemistry via [10.1039/C6DT04016K](https://doi.org/10.1039/C6DT04016K)

University of Bath

Alternative formats

If you require this document in an alternative format, please contact:
openaccess@bath.ac.uk

General rights

Copyright and moral rights for the publications made accessible in the public portal are retained by the authors and/or other copyright owners and it is a condition of accessing publications that users recognise and abide by the legal requirements associated with these rights.

Take down policy

If you believe that this document breaches copyright please contact us providing details, and we will remove access to the work immediately and investigate your claim.

Synthesis and Characterization of Phosphorescent Two-Coordinate Copper(I) Complexes Bearing Diamidocarbene Ligands

Shuyang Shi,^a Lee R. Collins,^b Mary F. Mahon,^b Peter I. Djurovich,^a
Mark E. Thompson^{*a} and Michael K. Whittlesey^{*b}

Abstract

The photophysical properties of four, two-coordinate, linear diamidocarbene copper(I) complexes, [(DAC)₂Cu][BF₄] (**1**), (DAC)CuOSiPh₃ (**2**), (DAC)CuC₆F₅ (**3**) and (DAC)Cu(2,4,6-Me₃C₆H₂) (**4**) (DAC = 1,3-bis(2,4,6-trimethylphenyl)-5,5-dimethyl-4,6-diketopyrimidinyl-2-ylidene) have been investigated. Complex **1** shows a high photoluminescence quantum efficiency (Φ_{PL}) in both the solid state ($\Phi_{\text{PL}} = 0.85$) and in CH₂Cl₂ solution ($\Phi_{\text{PL}} = 0.65$). The emission band of **1**, both as a crystalline solid and in solution, is narrow (fwhm = 2300 cm⁻¹) relative to the emission bands of **2** (fwhm = 2900 cm⁻¹) and **3** (fwhm = 3700 cm⁻¹). Complexes **2** and **3** are each brightly luminescent in the solid state ($\Phi_{\text{PL}} = 0.62$ and 0.18, respectively), but markedly less so in CH₂Cl₂ solution ($\Phi_{\text{PL}} = 0.03$ and < 0.01, respectively). Complex **4** is not emissive in either the solid state or in solution. Phosphorescence of **1** in CH₂Cl₂ solution shows negligible quenching by oxygen in CH₂Cl₂ solution. This insensitivity to quenching is attributed to the excited state redox potential being insufficient for electron transfer to oxygen.

Introduction

Phosphorescent Cu(I) complexes have received a great deal of attention for their use in applications including organic light emitting diodes (OLEDs),¹⁻⁴ solar-energy conversion,^{5, 6} sensors,⁷⁻⁹ and biological systems.^{10, 11} In the case of OLEDs, Cu(I) complexes have been considered as potential alternatives to the successful phosphorescent emitters using noble-metals¹²⁻¹⁴ due to the low cost of copper relative to such elements as iridium and platinum.^{1, 15, 16} The most extensively studied mononuclear luminescent Cu(I) complexes are four-coordinate tetrahedral homo- and heteroleptic complexes bearing diimine and organophosphine ligands.¹⁷⁻²² Recently, a variety of three-coordinate luminescent Cu(I) complexes bearing N-heterocyclic carbene (NHC) ligands have also been reported.²³⁻²⁷ Interestingly, while the catalytic properties of two-coordinate (NHC)Cu(I) complexes have been investigated extensively,²⁸⁻³⁵ reports of their luminescent properties have only appeared recently.^{36, 37} This oversight may be due to a previous belief that three and four-coordinate geometries at the copper center are required for efficient luminescence.^{21, 23, 38-43}

In this work, we have investigated four linear diamidocarbene Cu(I) complexes (Figure 1), the previously reported [(DAC)₂Cu][BF₄] (**1**)³⁰ and (DAC)Cu(2,4,6-Me₃C₆H₂) (**4**),⁴⁴ and two new compounds, (DAC)CuOSiPh₃ (**2**) and (DAC)CuC₆F₅ (**3**) (DAC = 1,3-bis(2,4,6-trimethylphenyl)-5,5-dimethyl-4,6-diketopyrimidinyl-2-ylidene). Diamidocarbenes display a combination of reduced σ -donor and greater π -acceptor properties relative to their diamino counterparts.⁴⁵⁻⁴⁸ We show that the bis(diamidocarbene) complex **1** exhibits high photoluminescence quantum efficiency in CH₂Cl₂ solution and its phosphorescence is

only weakly quenched under aerobic conditions, which differs from most other luminescent Cu(I) complexes.⁷⁻⁹ (Figure 1).

Results and Discussion

Synthesis and X-ray structures

Complexes **1** and **4** were synthesized according to literature procedures.^{30, 44} Complexes **2** and **3** were formed by protonolysis of either (DAC)CuO^tBu or **4** with Ph₃SiOH or C₆F₅H and isolated in 86% and 53% yield, respectively. Whereas the formation of **2** took place rapidly (<1 h) at room temperature, protonolysis with pentafluorobenzene required heating to 333 K for ca. 12 h, reflecting the higher acidity of the silanol (Ph₃SiOH, pK_a = 10.8;⁴⁹ C₆F₅H, pK_a = 24.2).⁵⁰ Complex **1** is indefinitely stable to air, whereas **2–4** are each air- and moisture-sensitive in solution and the solid state.

Single crystals of the compounds suitable for X-ray diffraction studies were grown from CH₂Cl₂/hexane (**1**), toluene/hexane (**2**) or by slow evaporation of arene/hexane solutions (**3** and

4) to afford the molecular structures shown in

Figure 2. The crystal structure of [(DAC)₂Cu]⁺

is for [(DAC)₂Cu][PF₆].⁴⁸ The photophysical

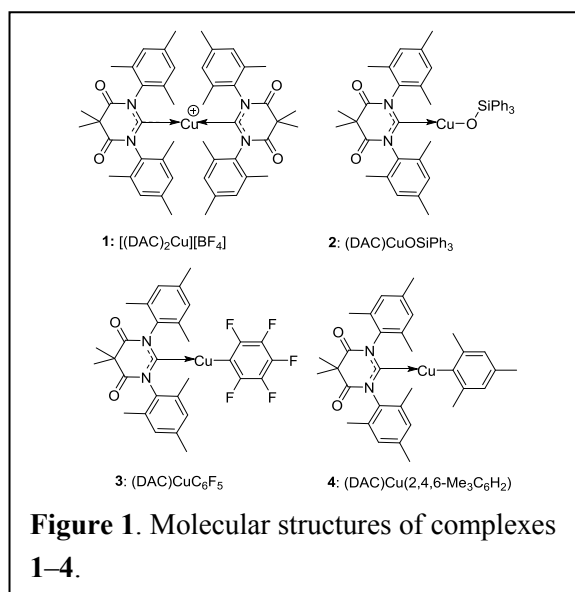
studies discussed below were carried out with

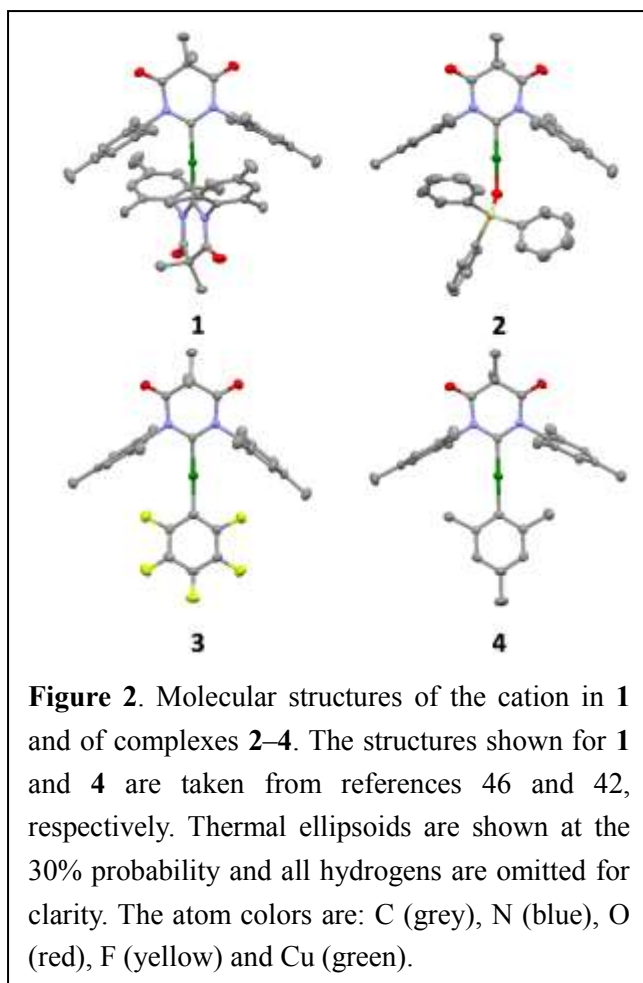
[(DAC)₂Cu][BF₄], but we do not expect the

structure of the (DAC)₂Cu⁺ ion to be dependent

on the identity of the counter ion. Compounds

1–4 all have monomeric, two-coordinate





structures with a linear geometry around the copper center (**1**: $178.4(1)^\circ$;⁴⁸ **2**: $178.8(1)^\circ$; **3**: $175.4(1)^\circ$; **4**: $179.7(1)^\circ$).⁴⁴

The Cu–C_{NHC} bond lengths in **1** ($1.926(2)$ Å and $1.927(2)$ Å)⁴⁸, **2** ($1.858(2)$ Å), **3** ($1.902(3)$ Å), and **4** ($1.905(3)$ Å)⁴⁴ are comparable to the values reported for diaminocarbene Cu(I) complexes.^{23, 24, 35, 51, 52} The significantly longer Cu–C_{NHC} distances in **1**, **3** and **4** compared to that of **2** and (DAC)CuCl ($1.886(2)$ Å)⁴⁸ are consistent with added

steric repulsion arising from the presence of a second carbene ligand or a 2,6-disubstituted aryl group.

The torsion angle between the planes of the two carbene ligands in complex **1** (defined as the angle between the N–C–N planes of the DAC ligands = 71°) is close to values found in other [(NHC)₂Cu]⁺ complexes bearing bulky N-aryl-substituted carbenes.^{30, 35, 51, 53} For complex **2**, the Cu–O–Si angle ($133.5(1)^\circ$) and the torsion angle between the carbene ligand and Cu–O–Si plane (76°) are both similar to those found for (IPr)CuOSiMe₂Ph (IPr = 1,3-bis(2,6-diisopropylphenyl)imidazol-2-ylidene).⁵² In contrast to the approximately perpendicular ligand planes in **1** and **2**, the copper bound aryl groups in complexes **3** and **4** are

nearly coplanar with the diamidocarbenes, having respective dihedral angles of 12° and 7°. The Cu–C₆F₅ distance (1.922(3) Å) in complex **3** is significantly longer than that in (py)CuC₆F₅ (Cu–C₆F₅ = 1.891(2) Å),⁵⁴ but shorter than in three-coordinate (IPr)Cu(tfppy) (Cu–C₆F₅ = 1.969(5) Å, tfppy = 2-(2,3,4,5-tetrafluorophenyl)pyridine).³⁸ The Cu–C(mesityl) distance of 1.927(3) Å in complex **4** is comparable to the values found in (iPr₂Me₂)Cu(2,4,6-Me₃C₆H₂) (1.922(4) Å, iPr₂Me₂ = 1,3-di-isopropyl-4,5-dimethylimidazol-2-ylidene)⁵⁵ and (IPr)Cu(2-MeOC₆H₄) (1.9155(18) Å).⁵⁶

Photophysical properties

Absorption spectra for complexes **1–4** in CH₂Cl₂ are shown in Figure 3, data is given in Table 1. Strong bands in the UV region ($\lambda < 300$ nm) are assigned to π - π^* transitions on the ligands. Absorption bands at lower energy are assigned to charge transfer (CT) transitions as

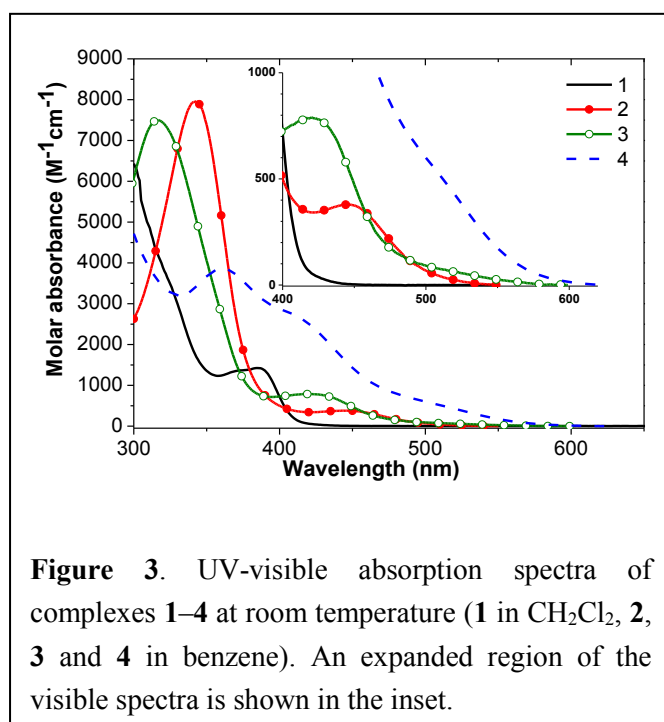


Figure 3. UV-visible absorption spectra of complexes **1–4** at room temperature (**1** in CH₂Cl₂, **2**, **3** and **4** in benzene). An expanded region of the visible spectra is shown in the inset.

they are absent in the free ligands. Relatively intense bands between 300–400 nm in **1** ($\epsilon = 1.4 \times 10^3 \text{ M}^{-1}\text{cm}^{-1}$) and **2** and **3** ($\epsilon > 7 \times 10^3 \text{ M}^{-1}\text{cm}^{-1}$), including those between 350–450 nm in **4**, are tentatively assigned to singlet metal-to-ligand charge transfer (¹MLCT) transitions. Bands with lower intensity ($\epsilon < 1 \times 10^3 \text{ M}^{-1}\text{cm}^{-1}$) at lower energy are

Table 1. Absorption data for complexes 1–4 .	
	$\lambda_{\text{max}}(\text{nm})$ (ϵ , $10^3 \text{ M}^{-1} \text{ cm}^{-1}$)
1	325sh (3.58), 375 (1.37), 385 (1.42)
2	343 (7.96), 447 (0.38)
3	317 (7.50), 420 (0.79)
4	361 (3.86), 410sh (2.73), 510sh (0.52)

^a Absorption spectra recorded in CH_2Cl_2 .

assigned to CT states with ligand-to-ligand character. Weak shoulders ($\epsilon < 2 \times 10^2 \text{ M}^{-1} \text{ cm}^{-1}$) at the lowest energies of these CT bands likely correspond to triplet CT states admixed with

states having significant singlet character (Figure 3, inset). The bands at energies between 400–550 nm for complexes **2–4** can be assigned to charge transfer (CT) transitions involving the non-carbene ligands since no equivalent low energy absorption features are present in the bis-carbene complex **1**.

Emission spectra for complexes **1–3** in the solid state and in solution are shown in Figure 4, and the photophysical data are summarized in Table 2. In the solid state, complex **1** gives bright blue emission, **2** and **3** display yellow-green emission and **4** is non-emissive. The full width half maximum (fwhm) value for the emission band of solid **1** is narrower (fwhm = 2300 cm^{-1}) than that of **2** (fwhm = 2900 cm^{-1}) and **3** (fwhm = 3700 cm^{-1}). The long lifetimes ($\tau > 10 \mu\text{s}$) found for the three compounds as either neat solids or in frozen solution can be fit to single exponential decays and are indicative of emission (phosphorescence) from triplet excited states. The broad emission bands of **2** and **3** are consistent with luminescence from a triplet charge transfer (^3CT) state, whereas the narrower profile in **1** is indicative of a greater degree of intraligand (^3IL) character in the excited state. There is a less than two-fold increase in emission lifetimes upon cooling the solid samples to 77 K, suggesting that thermally activated delayed fluorescence (TADF) does not contribute significantly to the luminescent

properties of these complexes.²⁵

The photoluminescent quantum efficiency (Φ_{PL}) of complexes **1–3** are quite high in the solid state, reaching 0.85 for **1** and 0.18 for **3**. The variation in Φ_{PL} follows the trend in radiative rate constants (k_r), which decrease in the order **1** > **2** > **3**, whereas the nonradiative rate constants (k_{nr}) increase in the order **1** < **2** < **3**. The trend in k_r indicates that **1** has the greatest amount of perturbing singlet character in its triplet state, whereas **3** has the lowest amount. The increase in k_{nr} from **1** to **2** can be a consequence of following Energy Gap Law

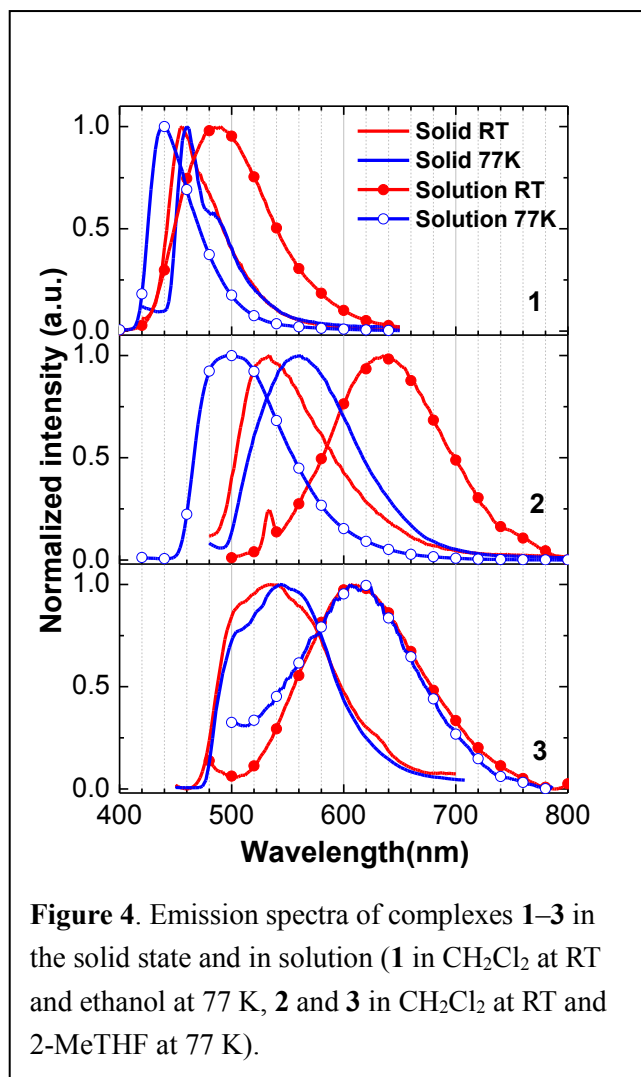


Figure 4. Emission spectra of complexes **1–3** in the solid state and in solution (**1** in CH_2Cl_2 at RT and ethanol at 77 K, **2** and **3** in CH_2Cl_2 at RT and 2-MeTHF at 77 K).

behavior;^{57, 58} however, the larger increase in **3** appears to be caused to additional nonradiative decay processes in the compound. The emission profiles for **1** and **3** in the solid state do not change markedly upon cooling to 77 K, whereas the spectrum for **2** broadens and undergoes a 28 nm red-shift. In contrast, the emission spectra for all three compounds broaden and undergo large bathochromic shifts ($\Delta\lambda_{\text{max}}$) in CH_2Cl_2 solution at room temperature ($\Delta\lambda_{\text{max}} = 34$ nm, 1500 cm^{-1} for **1**, $\Delta\lambda_{\text{max}} = 102$ nm, 3000 cm^{-1} for **2** and $\Delta\lambda_{\text{max}} = 72$ nm, 2200 cm^{-1} for **3**). The emission spectra are weakly solvatochromic: compound **1** displays a 10 nm hypsochromic shift

in polar CH₃CN, whereas **2** and **3** undergo bathochromic shifts of 16 nm and 22 nm, respectively, in non-polar benzene (Figures S17–19, ESI). The hypsochromic shifts in solvents with high polarity (CH₃CN for **1**, CH₂Cl₂ for **2** and **3**) indicate that the excited state is destabilized, and thus less polar, than the ground state.

Solution studies at low temperature were performed in ethanol for **1** as the compound was insoluble in 2-methyltetrahydrofuran (2-MeTHF), whereas **2** and **3**, while non-emissive in 2-MeTHF at room temperature, are strongly emissive in the same solvent at 77 K. The emission spectra in solution for both **1** and **2** display large hypsochromic shifts (50 nm for **1** and 140 nm for **2**) upon cooling to 77 K, whereas the spectrum for **3** is relatively unchanged. The rigidochromic shifts in **1** and **2** indicate that both compounds undergo large conformation changes in frozen media. In contrast, the structure of compound **3** is effectively unchanged in both fluid and rigid solvent. A structural change that can account for these differing behaviors is rotation of the ligand around the Cu–ligand bond axis. Examination of the X-ray crystal structures (Figure 2) shows the aryl rings of adjacent ligands in **1** and **2** can have close contact if both ligands are allowed to freely rotate. Therefore, significant structural changes caused by steric conflicts between opposing ligands can be expected when either complex is dissolved in fluid media. However, the C₆F₅ group in **3** presents a small degree of steric hindrance with respect to the adjacent DAC ligand, and thus only minor distortion is likely to occur amongst the various rotational conformers in the complex.

The luminescent efficiency for both complexes **2** and **3** are also much lower in solution (**2**; $\Phi_{\text{PL}} = 0.03$, **3**; $\Phi_{\text{PL}} < 0.01$) compared to **1**, which surprisingly remains highly emissive ($\Phi_{\text{PL}} =$

Table 1. Luminescent properties of complexes 1–3 in the solid state and solution. ^a												
Solid at room temperature						Solid at 77 K		Solution at room temperature ^b			Solution at 77 K ^c	
λ_{max} (nm)	τ (μs) ^d	Φ_{PL} ^e	k_r (10^4 s^{-1})	k_{nr} (10^4 s^{-1})		λ_{max} (nm)	τ (μs) ^d	λ_{max} (nm)	τ (μs) ^d	Φ_{PL} ^e	λ_{max} (nm)	τ (μs) ^d
1	456	18	0.85	4.7	0.83	460	19	490	18	0.65	440	20
2	534	16	0.62	3.9	2.4	562	20	636	1.2	0.03	496	16
3	534	12	0.18	1.5	6.8	543	13	606	0.37	<0.01	606	17

^a Complex **4** is non-emissive in either solid state or solution. ^b Recorded in CH_2Cl_2 .
^c Complex **1** recorded in ethanol, **2** and **3** in 2-MeTHF. ^d Error in τ is $\pm 5\%$. ^e Error in Φ_{PL} is $\pm 10\%$.

0.65). Copper(I) complexes generally have a significantly higher quantum efficiency as crystalline solids than in fluid solution.^{21, 40, 42, 59} The geometry of the compound is held rigidly in place in a crystalline sample, whereas structural relaxation in the excited state can occur more easily in fluid solution leading to both red shifted emission and enhanced non-radiative decay. Mononuclear Cu complexes having $\Phi_{\text{PL}} > 0.40$ in fluid solution are rare with only a few examples being previously reported.^{1, 16}

To obtain a better understanding of the outstanding photophysical behavior of complex **1** in fluid solution, a space filling model of the geometry optimized structures for **1** is shown in Figure 5. The steric encumbrance imposed by the 1,3,5- $\text{Me}_3\text{C}_6\text{H}_2$ rings on the N-substituents of the carbene ligands in **1**, in particular the ortho methyl groups, “lock” the aryl rings into positions orthogonal to the N–C–N plane of the diamidocarbene, effectively minimizing excited state deactivation caused by librational motion of the aryl rings. The rigidity of **1** leads

to only a minor decrease in non-radiative decay in fluid solution and a small red-shift in emission.

Further evidence of the significant steric crowding in **1** is provided by the luminescent quenching behaviour in MeCN solution. While the emission efficiency and lifetime are strongly diminished in MeCN ($\Phi_{\text{PL}} = 0.04$, $\tau = 1.1 \mu\text{s}$), the quenching rate constant determined by Stern-Volmer analysis for MeCN in CH_2Cl_2 is extremely small ($k_{\text{q}} = 3.8 \times 10^4 \text{ M}^{-1}\text{s}^{-1}$) compared to the value found for the *four*-coordinate Cu(I) complex $[\text{Cu}(\text{dmp})_2]^+$ ($k_{\text{q}} = 1.8 \times 10^7 \text{ M}^{-1}\text{s}^{-1}$, (dmp = 2,9-dimethyl-1,10-phenanthroline)).⁶⁰ The high quenching rate constants of bis(1,10-phenanthroline) Cu(I) complexes in Lewis basic solvents such as MeCN has been proposed to be due to formation of an exciplex involving direct coordination of the solvent to the metal center, which is expected to be precluded in **1**.^{42, 59, 61, 62} However, recent work has questioned the strength and nature of this copper-MeCN interaction and has instead attributed the luminescent quenching to the effect of outer-sphere solvation on the ³MLCT energy.^{63, 64} Regardless, the roughly thousand fold smaller value for the quenching rate constant of **1** by MeCN relative to that of $[\text{Cu}(\text{dmp})_2]^+$ implies effective steric protection of the copper complex by the DAC ligands.

A commonly cited application for phosphorescent copper complexes is as oxygen sensors, due to the high propensity for oxygen to quench their emission.⁷⁻⁹ Thus,

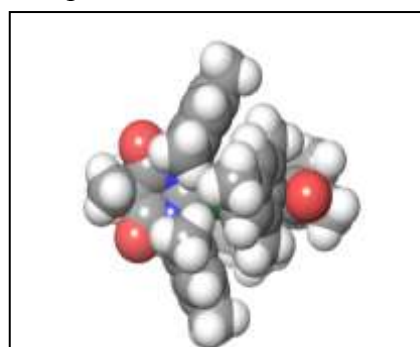


Figure 5. Space filling model of complex **1**. The model is obtained from geometry optimization using DFT calculations. Atom colors are: C (grey), H (white), N (blue), O (red) and Cu (green).

a decrease in the luminescent efficiency or lifetime of the complex in a given environment relative to the same complex under anaerobic conditions can be used to quantify the amount of oxygen present. Surprisingly, phosphorescence for **1** is only slightly decreased ($\Phi_{\text{PL}} = 0.50$) when a CH_2Cl_2 solution is sparged with O_2 . Similarly, the luminescent lifetime under nitrogen ($\tau = 18 \mu\text{s}$) is only slightly diminished in oxygenated CH_2Cl_2 ($\tau = 14 \mu\text{s}$). This relative insensitivity of the emission intensity and lifetime to oxygen is highly unusual for phosphorescent compounds. There are two possible quenching mechanisms of the triplet excited state by oxygen, involving either electron transfer or energy transfer.⁶⁵ For luminescent quenching by electron transfer (eq 1a) to be thermodynamically feasible, the excited state of **1** has to have a sufficient potential for oxidative quenching to be exergonic (eq 1b):



$$\Delta G = -nF[E(\text{O}_2^{0/-1}) - E(\mathbf{1}^{2+/1+*})] \quad 1b$$

Work terms needed to account for coulombic attraction/repulsion between the products and reactants in eq 1b should also be considered, but these values are typically small in solvents with high dielectric constants and for purposes of discussion here will be neglected. The value for $E(\mathbf{1}^{2+/1+*})$ in eq 1b is usually obtained by subtracting the spectroscopic excited state energy from the oxidation potential i.e. [$E(\mathbf{1}^{2+/1+*}) = E(\mathbf{1}^{2+/1+}) - E_{0-0}$]. Unfortunately, we were unable to obtain a value for $E(\mathbf{1}^{2+/1+})$ as we could not observe a discernible oxidation wave for **1** using cyclic voltammetry in MeCN. However, two distinct reversible reduction waves are present at $E^{1/2} = -1.48 \text{ V}$ and -1.78 V versus Fc^+/Fc ($\text{Fc} = \text{ferrocene}$), thus allowing a limiting value for

the thermodynamic potential for quenching by electron transfer to oxygen to be approximated using eqs 2a-b:



$$\Delta G = -nF[E(\text{O}_2^{0/-1}) - E(\mathbf{1}^{1+/0})] \quad 2b$$

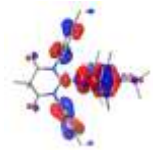
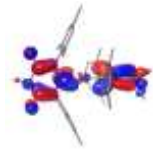

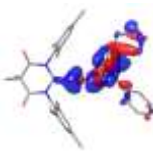
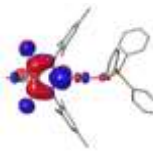

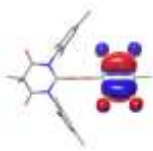
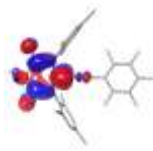
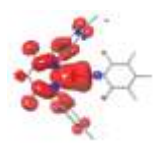
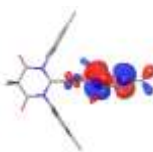
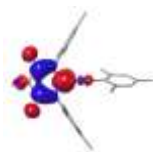

Using the reported value of $E(\text{O}_2^{0/-1})$ in MeCN (-1.29 V vs Fc^+/Fc)⁶⁶ in eq 2b gives an exergonic free energy ($\Delta G = -0.21$ V). However, a substantial increase in this free energy will be present when quenching $\mathbf{1}^*$ since a significant coulombic attraction needs to be accounted for in the removal of an electron from $\mathbf{1}^+$ (eq 1b) as opposed to $\mathbf{1}^0$ (eq 2b). This change in coulombic interaction can be estimated from the difference between the standard redox couples Cu(II)/Cu(I) and Cu(I)/Cu(0) ($\Delta E = +0.36$ V).⁶⁷ Upon adding this value to eq 2b, electron transfer becomes endergonic and thus, quenching of $\mathbf{1}^*$ by O_2 (eq 1a) will be a thermodynamically unfavorable process. This leaves Dexter energy transfer from the triplet state to oxygen (forming singlet oxygen) as a potential quenching pathway. Efficient Dexter energy transfer requires good overlap between the frontier molecular orbitals of both species,⁶⁵ which is expected to be severely constrained due to the steric demands of the DAC. Therefore, we can conclude that the relative insensitivity of phosphorescent quenching of $\mathbf{1}$ by O_2 is due to the combined effects of the high oxidation potential of the complex along with steric protection of the metal center by the DAC ligands.

DFT and TD-DFT Calculations

Density functional theory (DFT) calculations were carried out for all of the diamidocarbene complexes using geometric parameters obtained from X-ray analyses as starting structures for **1–4**. The frontier molecular orbital (MO) surfaces calculated for **1–4** are shown in Figure 6. The lowest singlet and triplet vertical energies determined by time-dependent DFT (TD-DFT) calculations are given in Table 3. The optimized ground state structures of **1–4** have a linear coordination geometry at the copper center, with bond lengths that correlate well to the values from the X-ray structures. The torsion angles from the crystal

structure and the optimized geometry in complex **1** are similar (71° and 79° respectively), reflecting the steric constraints of the two DAC ligands. In contrast, the DFT optimized geometry of complex **2** fails to reproduce the large ligand-ligand torsion angle in the crystal structure (X-ray: 76° ; DFT: 56°). This mismatch between experimental and computational structures is also seen for complexes **3** and **4** and is attributed to steric repulsion between the phenylene and DAC ligands, leading to larger torsion angles in the optimized geometries

Figure 6. Frontier orbitals and triplet spin densities calculated for complexes **1–4**.

	HOMO	LUMO	Spin density
1	 -8.85 eV	 -4.97 eV	
2	 -5.90 eV	 -2.60 eV	
3	 -5.85 eV	 -2.66 eV	
4	 -4.86 eV	 -2.49 eV	

when compared to the experimental values measured in the crystal structures (**3**: 12°→24°, **4**: 7°→60°). The optimized structures of the T₁ states in **1**, **3** and **4** retain a linear coordination geometry at the copper center (S₀→T₁: **1**: 178°→179°, **3**: 175°→179°, **4**: 180°→178°). Compound **2** has a smaller angle around copper center in the T₁ state (S₀→T₁: 179°→156°). The Cu–C_{NHC} bond distances decrease ca. 0.05 Å in T₁ state of **1**, **3** and **4** and increase by 0.03 Å in **2**. The bond lengths to the other ligand get either similarly longer (**1** and **3**) or remain unchanged (**2** and **4**). The torsion angles between the ligands in the T₁ state remain unchanged in **1** and **4**, whereas the torsion angles decrease in **3** (78°→56°) and **4** (32°→24°). Interestingly in **4**, despite having a linear C_{NHC}–Cu–C_{Mes} coordination geometry, the mesityl ring is no longer linearly coordinated to Cu. Instead, the aryl ring is bent with a Cu–C_{Mes}–centroid_{Mes} angle of 160°.

For complexes **1–4**, the calculated LUMOs have essentially identical orbital character, consisting predominantly of π* orbitals on the diamidocarbene ligands mixed with *d*-orbitals on copper. However, variation of the non-carbene ligand has a pronounced effect on HOMO composition and orbital energy. For the three heteroleptic Cu(I) complexes, the HOMOs are mainly localized on the metal and the non-carbene ligands. The HOMO energies

Table 3. Lowest vertical energy transitions for complexes **1–4** determined from TD-DFT calculations.

Complex	transitions ^a	λ (nm)	<i>f</i>
1	S ₀ →S ₁	396	0.0058
	S ₀ →T ₁	430	0
2	S ₀ →S ₁	510	0.0032
	S ₀ →T ₁	561	0
3	S ₀ →S ₁	494	0.0021
	S ₀ →T ₁	540	0
4	S ₀ →S ₁	645	0.0049
	S ₀ →T ₁	703	0

^a Orbital contributions to each transition are given in the supplementary information.

of **2** and **3** are similar, but that of **4** is destabilized by 1.0 eV due to the strong electron-donating ability of the mesityl group. TD-DFT calculations of **1–4** show that the calculated wavelength of the $S_0 \rightarrow S_1$ transitions correlate well with the solution absorption onsets (Table 2). The calculations indicate that the lowest lying triplet transitions for complex **1** is intra-ligand charge transfer (ILCT) admixed with metal-to-ligand charge transfer (MLCT) transitions. The lowest lying triplet transitions for **2–4** are principally MLCT admixed with ligand-to-ligand charge transfer (LLCT) character. The calculated spin density surfaces for the triplet electronic configuration further reflect these same assignments for emissive state showing contours that are principally localized on the DAC ligand and metal center (Figure 6).

Conclusion

The photophysical properties of a series of four linear, two-coordinate diamidocarbene copper(I) complexes along with a bis-diaminocarbene salt have been investigated. Complex **1** are stable to air and moisture, whereas **2–4** are air- and moisture sensitive. The bis(diamidocarbene) complex **1** displays narrow emission band relative to the other three diamidocarbene species and has a high photoluminescence quantum yield in both the solid state and CH_2Cl_2 solution ($\Phi_{\text{PL}} = 0.85$ and 0.65 , respectively). The phosphorescence of **1** is only weakly quenched by O_2 , which is remarkable for a Cu phosphor with an 18 μsec lifetime. Complex **1** contains a sterically demanding ligand, suggests that the steric bulk of the ligands around Cu is an important factor in designing systems with increased photoluminescence efficiency and suppressed quenching by oxygen. These results echo observations on

mononuclear four-coordinate copper complexes,^{16, 21} where increasing the steric bulk of the ligands bound to copper limits the structural changes that occur in the excited state, thereby increasing the luminescence efficiency.

Experimental

Synthesis. All manipulations were carried out using standard Schlenk, high vacuum and glovebox techniques using dried and degassed solvents. Hexane and toluene (purified using an MBraun SPS solvent system) and benzene (refluxed over sodium dispersion) were all dried further over 3 Å molecular sieves and stored over potassium mirrors. THF was refluxed over sodium wire and stored over 3 Å molecular sieves. C₆D₆ was dried over potassium and vacuum transferred. NMR spectra were recorded on a Bruker Avance 500 MHz NMR spectrometer and referenced to δ 7.16 (¹H) and δ 128.0 (¹³C). ¹⁹F spectra were referenced to CFCl₃ at δ = 0.0. IR spectra were recorded as KBr discs on a Nicolet Nexus spectrometer. Elemental analyses were performed by the Elemental Analysis Service, London Metropolitan University, London, UK and Elemental Microanalysis Limited, Okehampton, Devon, UK. DAC,^{47, 68} [(DAC)₂Cu][BF₄] (**1**),³⁰ (DAC)CuO^tBu,⁴⁴ [Cu(2,4,6-Me₃C₆H₂)]_n⁶⁹ and (DAC)Cu(2,4,6-Me₃C₆H₂) (**4**)⁴⁴ were prepared according to literature methods.

Synthesis of (DAC)CuOSiPh₃ (2). A benzene (20 mL) solution of (DAC)CuO^tBu (0.455 g, 0.886 mmol) and Ph₃SiOH (0.273 g, 0.989 mmol) was stirred at room temperature for 1 h, with a yellow precipitate being generated very early in the reaction. The solvent was removed under reduced pressure, the yellow residue dissolved in a minimum amount of toluene

and reprecipitated by addition of hexane. The solid was cannula filtered, washed with hexane (20 mL) and dried *in vacuo*. Single crystals suitable for X-ray diffraction studies were grown from toluene/hexane. Yield: 0.543 g (86%). ^1H NMR: δ_{H} (C_6D_6 , 500 MHz, 298 K) 7.63 (m, 6H, *o*-SiArH), 7.19 (m, 9H, *m*-SiArH and *p*-SiArH), 6.68 (s, 4H, *m*-NArH), 2.05 (s, 6H, *p*-NArCH₃), 1.93 (s, 12H, *o*-NArCH₃), 1.30 (s, 6H, C(CH₃)₂). $^{13}\text{C}\{^1\text{H}\}$ NMR: δ_{C} (C_6D_6 , 126 MHz, 298 K) 216.0 (s, NCN), 171.2 (s, CO), 142.7 (s, *i*-SiAr), 139.8 (s, *p*-NAr), 136.0 (s, *i*-NAr), 135.5 (s, *o*-SiAr), 134.1 (s, *o*-NAr), 130.4 (s, *m*-NAr), 128.2 (s, *p*-SiAr), 127.3 (s, *m*-SiAr), 51.3 (s, OC(CH₃)₂), 24.3 (s, OC(CH₃)₃), 21.1 (s, *p*-NArCH₃), 18.0 (s, *o*-NArCH₃). IR (cm^{-1}): 1759 (ν_{CO}), 1729 (ν_{CO}). Analysis found: C, 70.45; H, 6.19; N, 4.00. C₄₂H₄₃N₂O₃SiCu requires: C, 70.51; H, 6.06; N, 3.92.

Synthesis of (DAC)CuC₆F₅ (3). C₆F₅H (0.150 mL, 1.35 mmol) was added to a benzene (10 mL) solution of (DAC)Cu(2,4,6-Me₃C₆H₂) (0.498 g, 0.89 mmol) in a rigorously flame dried ampoule and the mixture heated at 60 °C for 21 h. After cooling to room temperature, the solvent was removed and the dull orange residue dried *in vacuo*. This was washed with 20 mL of 1:4 v:v benzene/hexane mixture and then with hexane (3 x 10 mL) to give a bright orange powder after drying. Yield: 0.285 g (53%). Single crystals suitable for X-ray diffraction were grown by slow evaporation of a benzene/hexane solution (1:4 v:v). ^1H NMR: δ_{H} (C_6D_6 , 500 MHz, 298 K) 6.78 (s, 4H, *m*-NArH), 2.06 (s, 12H, *o*-NArCH₃), 2.05 (s, 6H, *p*-NArCH₃), 1.34 (s, 6H, C(CH₃)₂). $^{13}\text{C}\{^1\text{H}\}$ NMR: δ_{C} (C_6D_6 , 126 MHz, 298 K; signals for the C₆F₅ ligand were not observed) 216.8 (s, NCN), 171.3 (s, CO), 140.4 (s, *p*-NAr), 135.2 (s, *i*-NAr), 134.2 (s, *o*-NAr), 130.4 (s, *m*-NAr), 51.7 (s, C(CH₃)₂), 24.3 (s, C(CH₃)₂), 21.0 (s, *p*-NArCH₃), 18.2

(s, *o*-NArCH₃). ¹⁹F NMR: δ_F (C₆D₆, 470 MHz, 298 K) -112.5 (m, 2F, *o*-C₆F₅), -159.4 (t, ³J_{FF} = 20 Hz, 1F, *p*-C₆F₅), -163.0 (m, 2F, *m*-C₆F₅). IR (cm⁻¹): 1763 (ν_{CO}), 1732 (ν_{CO}). Analysis found: C, 59.21; H, 4.72; N, 4.64. C₃₀H₂₈N₂O₂F₅Cu requires: C, 59.35; H, 4.65; N, 4.61.

X-ray crystallography. An Agilent Supernova diffractometer equipped with Cu(Kα) X-rays was used for data collection on **2**, while a Nonius kappaCCD diffractometer equipped with Mo(Kα) X-rays was employed for data acquisition on **4**. Both experiments were conducted at 150 K. Crystal structure solution and refinement was unremarkable in both cases. CCDC 1480899 and 1480900 contain the supplementary crystallographic data for **2** and **4**, respectively. These data can be obtained free of charge at <http://www.ccdc.cam.ac.uk/conts/retrieving.html>, or from the Cambridge Crystallographic Data Centre, CCDC, 12 Union Road, Cambridge CB2 1EZ, UK (Fax: 44-1223-336-033; or E-Mail: deposit@ccdc.cam.ac.uk)

Density Functional Calculations. All calculations were performed using Jaguar 9.1 (release 13) software package on the Schrodinger Material Science Suite (v2016-1). Gas phase geometry optimization was calculated using B3LYP functional with the LACVP** basis set as implemented in Jaguar. Geometric parameters obtained from XRD analyses were used as a starting point for geometry optimization in the ground state and triplet state.

Photophysical Characterization. The UV-visible spectra were recorded on a Hewlett-Packard 4853 diode array spectrometer. Photoluminescent emission measurements were performed using a Photon Technology International QuantaMaster Model C-60 fluorimeter. Phosphorescent lifetimes were measured by time-correlated single-photon counting using an IBH Fluorocube instrument equipped with an LED excitation source.

Quantum yield measurements were carried out using a Hamamatsu C9920 system equipped with a xenon lamp, calibrated integrating sphere and model C10027 photonic multi-channel analyzer (PMA). All solid and solution samples were prepared in the glovebox prior to performing emission, lifetime, and quantum yield measurements.

Acknowledgements

We thank Universal Display Corporation and EPSRC/DTA for financial support.

Notes and References

^a Department of Chemistry, University of Southern California, Los Angeles, California 90089, USA. Email: met@usc.edu

^b Department of Chemistry, University of Bath, Claverton Down, Bath BA2 7AY, UK. Email: M.K.Whittlesey@bath.ac.uk

† Electronic supplementary information (ESI) available: ¹H spectra in C₆D₆ (**2**, **3** and **5**) and ¹⁹F NMR spectra of **3** in C₆D₆, DFT calculations including lowest vertical energy transitions for complexes **1-5** and atom positions for the optimized ground and triplet excited states. CCDC 1480899 and 1480900. For ESI and crystallographic data in CIF or other electronic format see DOI:

1. M. Hashimoto, S. Igawa, M. Yashima, I. Kawata, M. Hoshino and M. Osawa, *Journal of the American Chemical Society*, 2011, **133**, 10348-10351.
2. F. Wu, J. Li, H. Tong, Z. Li, C. Adachi, A. Langlois, P. D. Harvey, L. Liu, W.-Y. Wong, W.-K. Wong and X. Zhu, *Journal of Materials Chemistry C*, 2015, **3**, 138-146.
3. F. Wei, J. Qiu, X. Liu, J. Wang, H. Wei, Z. Wang, Z. Liu, Z. Bian, Z. Lu, Y. Zhao and C. Huang, *Journal of Materials Chemistry C*, 2014, **2**, 6333-6341.
4. D. Volz, Y. Chen, M. Wallesch, R. Liu, C. Fléchon, D. M. Zink, J. Friedrichs, H. Flügge, R. Steininger, J. Göttlicher, C. Heske, L. Weinhardt, S. Bräse, F. So and T. Baumann, *Advanced Materials*, 2015, **27**, 2538-2543.
5. S. Hattori, Y. Wada, S. Yanagida and S. Fukuzumi, *Journal of the American Chemical Society*, 2005, **127**, 9648-9654.
6. M. Magni, R. Giannuzzi, A. Colombo, M. P. Cipolla, C. Dragonetti, S. Caramori, S. Carli, R. Grisorio, G. P. Suranna, C. A. Bignozzi, D. Roberto and M. Manca, *Inorganic Chemistry*, 2016, **55**, 5245-5253.
7. C. S. Smith, C. W. Branham, B. J. Marquardt and K. R. Mann, *Journal of the American*

- Chemical Society*, 2010, **132**, 14079-14085.
8. L. Guangying and F. Jun, *Sensors and Actuators B: Chemical*, 2016, **233**, 347-354.
 9. X.-y. Xu, H.-n. Xiao and A.-p. Deng, *Optical Materials*, 2014, **36**, 1542-1554.
 10. D. R. McMillin and K. M. McNett, *Chemical Reviews*, 1998, **98**, 1201-1220.
 11. S. Mahadevan and M. Palaniandavar, *Inorganic Chemistry*, 1998, **37**, 693-700.
 12. H. Yersin and D. Donges, in *Transition Metal and Rare Earth Compounds: Excited States, Transitions, Interactions II*, ed. H. Yersin, Springer Berlin Heidelberg, Berlin, Heidelberg, 2001, pp. 81-186.
 13. M. A. Baldo, D. F. O'Brien, Y. You, A. Shoustikov, S. Sibley, M. E. Thompson and S. R. Forrest, *Nature*, 1998, **395**, 151-154.
 14. Z. He, W.-Y. Wong, X. Yu, H.-S. Kwok and Z. Lin, *Inorganic Chemistry*, 2006, **45**, 10922-10937.
 15. D. G. Cuttell, S.-M. Kuang, P. E. Fanwick, D. R. McMillin and R. A. Walton, *Journal of the American Chemical Society*, 2002, **124**, 6-7.
 16. A. J. M. Miller, J. L. Dempsey and J. C. Peters, *Inorganic Chemistry*, 2007, **46**, 7244-7246.
 17. D. V. Scaltrito, D. W. Thompson, J. A. O'Callaghan and G. J. Meyer, *Coordination Chemistry Reviews*, 2000, **208**, 243-266.
 18. N. Armaroli, G. Accorsi, F. Cardinali and A. Listorti, in *Photochemistry and Photophysics of Coordination Compounds I*, eds. V. Balzani and S. Campagna, Springer Berlin Heidelberg, Berlin, Heidelberg, 2007, pp. 69-115.
 19. C.-W. Hsu, C.-C. Lin, M.-W. Chung, Y. Chi, G.-H. Lee, P.-T. Chou, C.-H. Chang and P.-Y. Chen, *Journal of the American Chemical Society*, 2011, **133**, 12085-12099.
 20. S. Igawa, M. Hashimoto, I. Kawata, M. Yashima, M. Hoshino and M. Osawa, *Journal of Materials Chemistry C*, 2013, **1**, 542-551.
 21. C. L. Linfoot, M. J. Leidl, P. Richardson, A. F. Rausch, O. Chepelin, F. J. White, H. Yersin and N. Robertson, *Inorganic Chemistry*, 2014, **53**, 10854-10861.
 22. R. Czerwieńiec and H. Yersin, *Inorganic Chemistry*, 2015, **54**, 4322-4327.
 23. V. A. Krylova, P. I. Djurovich, J. W. Aronson, R. Haiges, M. T. Whited and M. E. Thompson, *Organometallics*, 2012, **31**, 7983-7993.
 24. V. A. Krylova, P. I. Djurovich, B. L. Conley, R. Haiges, M. T. Whited, T. J. Williams and M. E. Thompson, *Chemical Communications*, 2014, **50**, 7176-7179.
 25. M. J. Leidl, V. A. Krylova, P. I. Djurovich, M. E. Thompson and H. Yersin, *Journal of the American Chemical Society*, 2014, **136**, 16032-16038.
 26. R. Visbal and M. C. Gimeno, *Chemical Society Reviews*, 2014, **43**, 3551-3574.
 27. R. Marion, F. Sguerra, F. Di Meo, E. Sauvageot, J.-F. Lohier, R. Daniellou, J.-L. Renaud, M. Linares, M. Hamel and S. Gaillard, *Inorganic Chemistry*, 2014, **53**, 9181-9191.
 28. S. Díez-González, N. Marion and S. P. Nolan, *Chemical Reviews*, 2009, **109**, 3612-3676.
 29. F. Lazreg, F. Nahra and C. S. J. Cazin, *Coordination Chemistry Reviews*, 2015, **293-294**, 48-79.

30. L. R. Collins, T. M. Rookes, M. F. Mahon, I. M. Riddlestone and M. K. Whittlesey, *Organometallics*, 2014, **33**, 5882-5887.
31. L. Zhan, R. Pan, P. Xing and B. Jiang, *Tetrahedron Letters*, 2016, **57**, 4036-4038.
32. S. Guo, M. H. Lim and H. V. Huynh, *Organometallics*, 2013, **32**, 7225-7233.
33. F. Lazreg, A. M. Z. Slawin and C. S. J. Cazin, *Organometallics*, 2012, **31**, 7969-7975.
34. S. Díez-González and S. P. Nolan, *Angewandte Chemie International Edition*, 2008, **47**, 8881-8884.
35. S. Díez-González, E. D. Stevens, N. M. Scott, J. L. Petersen and S. P. Nolan, *Chemistry – A European Journal*, 2008, **14**, 158-168.
36. M. Gernert, U. Müller, M. Haehnel, J. Pflaum and A. Steffen, *Chemistry – A European Journal*, 2016, n/a-n/a.
37. A. S. Romanov, D. Di, L. Yang, J. Fernandez-Cestau, C. R. Becker, C. E. James, B. Zhu, M. Linnolahti, D. Credgington and M. Bochmann, *Chemical Communications*, 2016, **52**, 6379-6382.
38. R. Molteni, K. Edkins, M. Haehnel and A. Steffen, *Organometallics*, 2016, **35**, 629-640.
39. M. J. Leitzl, F.-R. Kuchle, H. A. Mayer, L. Wesemann and H. Yersin, *The Journal of Physical Chemistry A*, 2013, **117**, 11823-11836.
40. V. A. Krylova, P. I. Djurovich, M. T. Whited and M. E. Thompson, *Chemical Communications*, 2010, **46**, 6696-6698.
41. Z. A. Siddique, Y. Yamamoto, T. Ohno and K. Nozaki, *Inorganic Chemistry*, 2003, **42**, 6366-6378.
42. N. A. Gothard, M. W. Mara, J. Huang, J. M. Szarko, B. Rolczynski, J. V. Lockard and L. X. Chen, *The Journal of Physical Chemistry A*, 2012, **116**, 1984-1992.
43. K. A. Barakat, T. R. Cundari and M. A. Omary, *Journal of the American Chemical Society*, 2003, **125**, 14228-14229.
44. L. R. Collins, I. M. Riddlestone, M. F. Mahon and M. K. Whittlesey, *Chemistry – A European Journal*, 2015, **21**, 14075-14084.
45. J. P. Moerdyk, D. Schilter and C. W. Bielawski, *Accounts of Chemical Research*, 2016, **49**, 1458-1468.
46. T. W. Hudnall and C. W. Bielawski, *Journal of the American Chemical Society*, 2009, **131**, 16039-16041.
47. V. Cesar, N. Lugan and G. Lavigne, *European Journal of Inorganic Chemistry*, 2010, 361-365.
48. L. R. Collins, J. P. Lowe, M. F. Mahon, R. C. Poulten and M. K. Whittlesey, *Inorganic Chemistry*, 2014, **53**, 2699-2707.
49. R. Duchateau, U. Cremer, R. J. Harmsen, S. I. Mohamud, H. C. L. Abbenhuis, R. A. van Santen, A. Meetsma, S. K. H. Thiele, M. F. H. van Tol and M. Kranenburg, *Organometallics*, 1999, **18**, 5447-5459.
50. K. Uneyama, *Organofluorine Chemistry*, Blackwell Publishing, Oxford, 2006.
51. B. Bantu, D. Wang, K. Wurst and M. R. Buchmeiser, *Tetrahedron*, 2005, **61**, 12145-

- 12152.
52. C. Kleeberg, M. S. Cheung, Z. Lin and T. B. Marder, *Journal of the American Chemical Society*, 2011, **133**, 19060-19063.
 53. S. Díez-González, N. M. Scott and S. P. Nolan, *Organometallics*, 2006, **25**, 2355-2358.
 54. A. Sundararaman, L. N. Zakharov, A. L. Rheingold and F. Jakle, *Chemical Communications*, 2005, 1708-1710.
 55. M. Niemeyer, *Zeitschrift für anorganische und allgemeine Chemie*, 2003, **629**, 1535-1540.
 56. A. Ueno, M. Takimoto, W. W. N. O, M. Nishiura, T. Ikariya and Z. Hou, *Chemistry – An Asian Journal*, 2015, **10**, 1010-1016.
 57. J. V. Caspar and T. J. Meyer, *The Journal of Physical Chemistry*, 1983, **87**, 952-957.
 58. J. V. Caspar and T. J. Meyer, *Inorganic Chemistry*, 1983, **22**, 2444-2453.
 59. M. K. Eggleston, D. R. McMillin, K. S. Koenig and A. J. Pallenberg, *Inorganic Chemistry*, 1997, **36**, 172-176.
 60. C. E. A. Palmer, D. R. McMillin, C. Kirmaier and D. Holten, *Inorganic Chemistry*, 1987, **26**, 3167-3170.
 61. E. M. Stacy and D. R. McMillin, *Inorganic Chemistry*, 1990, **29**, 393-396.
 62. G. B. Shaw, C. D. Grant, H. Shirota, E. W. Castner, G. J. Meyer and L. X. Chen, *Journal of the American Chemical Society*, 2007, **129**, 2147-2160.
 63. T. J. Penfold, S. Karlsson, G. Capano, F. A. Lima, J. Rittmann, M. Reinhard, M. H. Rittmann-Frank, O. Braem, E. Baranoff, R. Abela, I. Tavernelli, U. Rothlisberger, C. J. Milne and M. Chergui, *The Journal of Physical Chemistry A*, 2013, **117**, 4591-4601.
 64. G. Capano, U. Rothlisberger, I. Tavernelli and T. J. Penfold, *The Journal of Physical Chemistry A*, 2015, **119**, 7026-7037.
 65. P. I. Djurovich, D. Murphy, M. E. Thompson, B. Hernandez, R. Gao, P. L. Hunt and M. Selke, *Dalton Transactions*, 2007, 3763-3770.
 66. P. S. Singh and D. H. Evans, *The Journal of Physical Chemistry B*, 2006, **110**, 637-644.
 67. A. J. Bard, R. Parsons and J. Jordan, *Standard Potentials in Aqueous Solutions*, Marcel Dekker, Inc., New York, 1985.
 68. T. W. Hudnall, J. P. Moerdyk and C. W. Bielawski, *Chemical Communications*, 2010, **46**, 4288-4290.
 69. H. Eriksson and M. Håkansson, *Organometallics*, 1997, **16**, 4243-4244.